

Supplementary Information

Abundant Active-sites Engineering Enables Porous Co-N-C Electro-catalyst with Superior Oxygen Reduction Reaction Activity

Yue Zhang^a, Zexuan Du^a, Huaping Mei^a, Bingye Song^{a,*}, Qianzhi Gou^{a,*}, Xiaolin Hu^{b,*}, Di Qi^a, Ran Gao^a, Xianda Sun^c

a. *International Joint Laboratory on Low Carbon Built Environment of MOE, School of Building Services Science and Engineering, Xi'an University of Architecture and Technology, Xi'an 710055, China*

b. *School of Science, Chongqing Key Laboratory of New Energy Storage Materials and Devices, Chongqing University of Technology, Chongqing 400054, China*

c. *Institute for Advanced Science and Technology, Shandong University, Jinan 250061, China*

* *Correspondent author, Email: bysong@xauat.edu.cn, gqz813@xauat.edu.cn, huxl@cqut.edu.cn*

Section 1: Experiments and Materials

Zinc nitrate hexahydrate ($\text{Zn}(\text{NO}_3)_2 \cdot 6\text{H}_2\text{O}$, >99.0%), Cobaltous nitrate hexahydrate ($\text{Co}(\text{NO}_3)_2 \cdot 6\text{H}_2\text{O}$, >99.0%), riboflavin ($\text{C}_{17}\text{H}_{20}\text{N}_4\text{O}_6$, >98%), and 2-methylimidazole (2-MEIM, >98%) of AR grade were purchased from Aladdin Industrial Corporation (Shanghai, China). Methanol (CH_3OH , AR) and ethanol ($\text{C}_2\text{H}_5\text{OH}$, AR) were provided by Tianjin Fuyu Fine Chemical Co (Tianjin, China). 20% Pt/C and Nafion solution (5%) were bought from Johnson Matthey Company and DuPont, respectively. All the chemicals were used as received without further purification.

Section 2: Physical Characterization

The surface morphology and internal structure of the prepared ORR catalysts were characterized using a field emission scanning electron microscope (SEM, Gemini 500,

Zeiss, Germany) and a field emission transmission electron microscope (**TEM, F200x, FEI Talos, USA**). A combination of high-angle annular dark field scanning transmission electron microscopy (**HAADF-STEM**) and energy-dispersive spectroscopy (**EDS**) was employed to conduct a detailed investigation of the elemental distribution within the samples.

Thermogravimetric analysis (**TGA**) of the samples was conducted using a **PerkinElmer STA 8000** thermal analyzer within a nitrogen atmosphere, across a temperature range of room temperature to 1000°C, at a heating rate of 10°C/min. The weight changes of the catalyst were measured as the temperature continuously varied.

X-ray diffraction (**XRD, Rigaku SmartLab SE, Japan**) was employed to provide precise insights into the crystallographic arrangement and parameters of the samples by measuring the diffraction angles and intensities.

X-ray photoelectron spectroscopy (**XPS, Thermo Scientific K-Alpha, USA**) was employed to accurately determine the chemical states, molecular structures, and chemical bonding information of the surface compounds of the materials. The C 1s peak (at an energy of 284.8 eV) was used as the reference for energy calibration.

Nitrogen adsorption/desorption isotherms were measured utilizing an automatic surface area and porosity analyzer (**Micromeritics ASAP 2460, USA**). The Brunauer-Emmett-Teller (BET) method was employed to calculate the specific surface area of the materials, while the Barrett-Joyner-Halenda (BJH) method was utilized to determine the pore size distribution based on the obtained data.

Fourier-transform infrared spectroscopy (**FTIR, Thermo Fisher Scientific Nicolet iS20, USA**) was employed to analyze the molecular absorption characteristics of infrared radiation. By examining the position, intensity, and shape of the spectral bands, the spatial conformations of the molecules were determined, and a qualitative analysis of the functional groups was conducted.

Raman spectroscopy (**Horiba LabRAM HR Evolution, Japan**) was employed for the analysis of the light scattering characteristics of the materials, thereby enabling the identification of the molecular structures and chemical compositions.

Section 3: Characterization of Electrochemical Performance

The electrochemical performance of the Co-N-C catalysts was evaluated in detail through cyclic voltammetry (CV) curves, linear sweep voltammetry (LSV) curves, electrochemical impedance spectroscopy (EIS), and chronopotentiometry. This assessment was conducted to evaluate their ORR catalytic activity, electron transfer resistance, and stability.

All electrochemical experiments conducted in this study were performed using a rotating ring-disc electrode (RRDE) setup under a three-electrode system with a 0.1 M KOH electrolyte solution. The working electrode was a glassy carbon rotating ring-disc electrode (**GC RRDE, Pine, USA**). A mercury/mercury oxide (Hg/HgO) electrode was used as the reference electrode and a carbon rod was served as the counter electrode in all measurements. The catalyst was prepared by mixing 4 mg of the catalyst with 500 μ L of ethanol, 500 μ L of deionized water, and 45 μ L of Nafion (**5% wt%, DuPont**) to form a homogeneous catalyst ink through sonication. Subsequently, 12.5 μ L of the catalyst ink was uniformly coated onto the surface of the working electrode, ensuring a catalyst loading of 196 μ g \cdot cm⁻². To assess the electrochemical performance of the catalyst, a commercial Pt/C working electrode (**20 wt%, Johnson Matthey**) with an identical loading was prepared as a control. All potential values referenced to the Hg/HgO electrode were converted to the reversible hydrogen electrode (RHE) potential using the following equation:

$$E(\text{RHE}) = E(\text{MMO}) + 0.0591 pH + 0.098 \quad \backslash *$$

MERGEFORMAT (1)

To preliminarily evaluate the oxygen reduction reaction activity of the Co-N-C catalyst, a cyclic voltammogram was performed in a 0.1 mol \cdot L⁻¹ KOH electrolyte under saturated N₂ and saturated O₂ atmospheres. The scanning rate was maintained at 50 mV \cdot s⁻¹, with a voltage range of -0.866 V to 0.334 V (vs. MMO).

In order to characterize the impedance characteristics of electron transfer during the catalysis of the oxygen reduction reaction (ORR) by the Co-N-C catalysts, electrochemical impedance spectroscopy (EIS) measurements were conducted in the kinetic control region at a potential of 0 V (vs. MMO). The frequency range for the

measurements was set from 100 kHz to 0.1 Hz, with an applied AC voltage amplitude of 10 mV.

Accelerated durability tests (ADT) were conducted on the Co-N-C catalysts. The testing parameters were set within a potential range of 0.6 to 1.0 V (versus the reversible hydrogen electrode, RHE), with a scan rate of 100 mV·s⁻¹, and were performed in an oxygen-saturated 0.1 M KOH solution for 1000 cycles. The stability of the Co-N-C catalysts was evaluated through a chronoamperometric (i-t) response analysis conducted over a 40,000-second period, with the discharge potential set at 0.65 V (vs. RHE). To further investigate the alcohol tolerance of the Co-N-C catalysts, a 3 mol·L⁻¹ methanol solution was added to the electrolyte at a discharge time of 300 seconds under the same testing conditions, and the discharge current data was recorded in real time.

To gain deeper insights into the ORR mechanism, linear sweep voltammetry (LSV) experiments were conducted in O₂-saturated 0.1 M KOH electrolyte at a scan rate of 10 mV·s⁻¹ under different rotation speeds (400, 625, 900, 1225, 1600, and 2025 rpm). The number of transferred electrons (*n*) was determined on the basis of the slope of the Koutecky-Levich equation, as illustrated in Equations (2) and (3).

$$\frac{1}{j} = \frac{1}{j_d} + \frac{1}{j_k} = \frac{1}{B\omega^{\frac{1}{2}}} + \frac{1}{j_k} \quad \backslash*$$

MERGEFORMAT (2)

$$B = 0.2nFC_0(D_0)^{\frac{2}{3}}\mu^{-\frac{1}{6}} \quad \backslash*$$

MERGEFORMAT (3)

Where *j* is the measured current density, *j_k* is the kinetic current density, *j_d* is the diffusion limiting current density, *ω* is the rotation speed, *F* is the Faraday constant (96485 C·mol⁻¹), *C₀* is the saturated concentration of O₂ (1.1×10⁻⁶ mol·cm⁻³), *D₀* is the diffusion coefficient of O₂ in the solution (1.9×10⁻⁵ cm²·s⁻¹), *μ* is the kinetic viscosity of the electrolyte (0.01cm²·s⁻¹), *n* is the overall number of electrons gained per O₂.

To accurately assess the byproduct yield and the number of transferred electrons, rotating ring-disk electrode (RRDE) tests were conducted at a rotation speed of 1600

rpm and a scanning rate of 10 mV·s⁻¹. The electron transfer number (n) and hydrogen peroxide (H₂O₂) yield were calculated using the following formulas:

$$n = 4 \frac{I_d}{I_d + I_r / N} \quad \backslash*$$

MERGEFORMAT (4)

$$H_2O_2(\%) = 200 \frac{I_r / N}{I_d + I_r / N} \quad \backslash*$$

MERGEFORMAT (5)

I_d and I_r represent the current densities at the disk and ring electrodes, respectively, and N denotes the collection efficiency of the Pt ring, set at 0.37.

The objective of this study was to investigate the correlation between the electrochemical catalytic efficiency and the electrochemical active surface area (ECSA) in oxygen reduction reactions. To this end, cyclic voltammetry (CV) curves were measured within a specific potential range (0.71-0.81 V vs. RHE) and at various scan rates (20-100 mV·s⁻¹). To ensure consistency in the comparison of catalyst activity, the data were normalized on the basis of the same active sites. Utilizing linear regression analysis, the double-layer capacitance (C_{dl}) value in a saturated N₂ atmosphere within a 0.1 M KOH electrolyte solution was calculated, and ECSA was derived in accordance with Equation (6).

$$ECSA = \frac{C_{dl}}{C_s} \quad \backslash*$$

MERGEFORMAT (6)

Where C_s is a value denoting the electrical conductivity of a flat surface of a given sample or substance, subject to identical electrolyte conditions. In this study, the value assigned to C_s is 0.06 mF·cm⁻².

Section 4: Charts and Diagrams

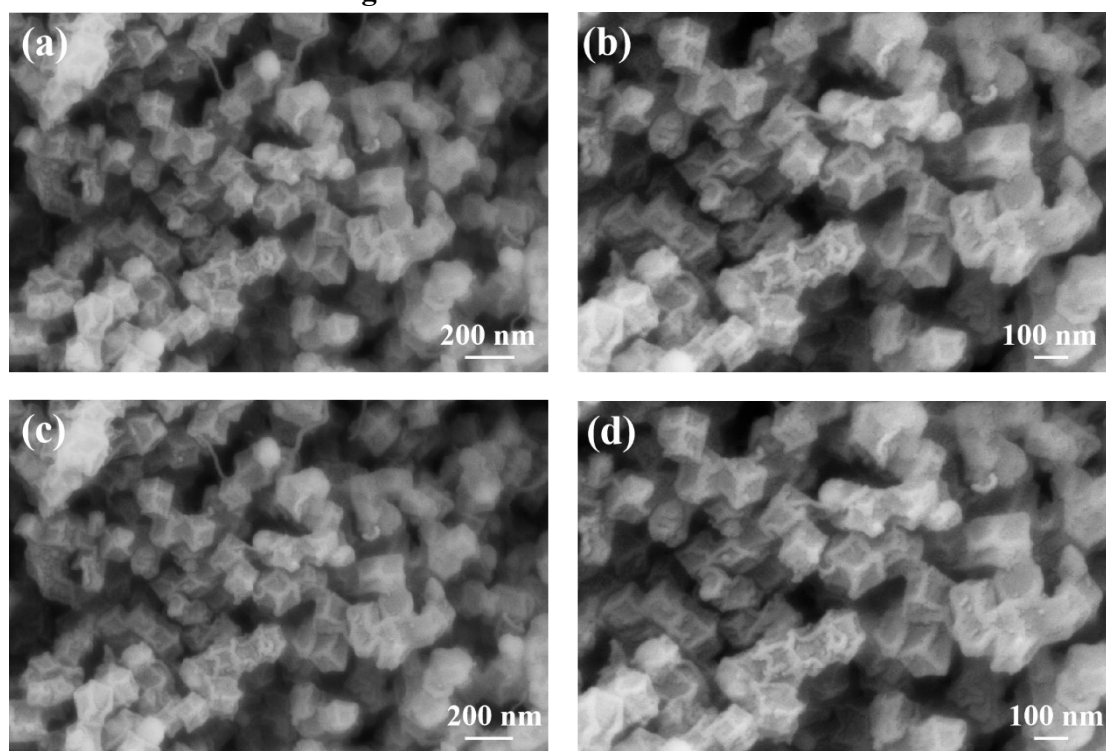


Figure S1. (a-b) SEM images of $\text{Co}_V\text{-N-C}_{750}$ electrode at different magnifications
(c-d) SEM images of $\text{Co}_V\text{-N-C}_{950}$ electrode at different magnifications

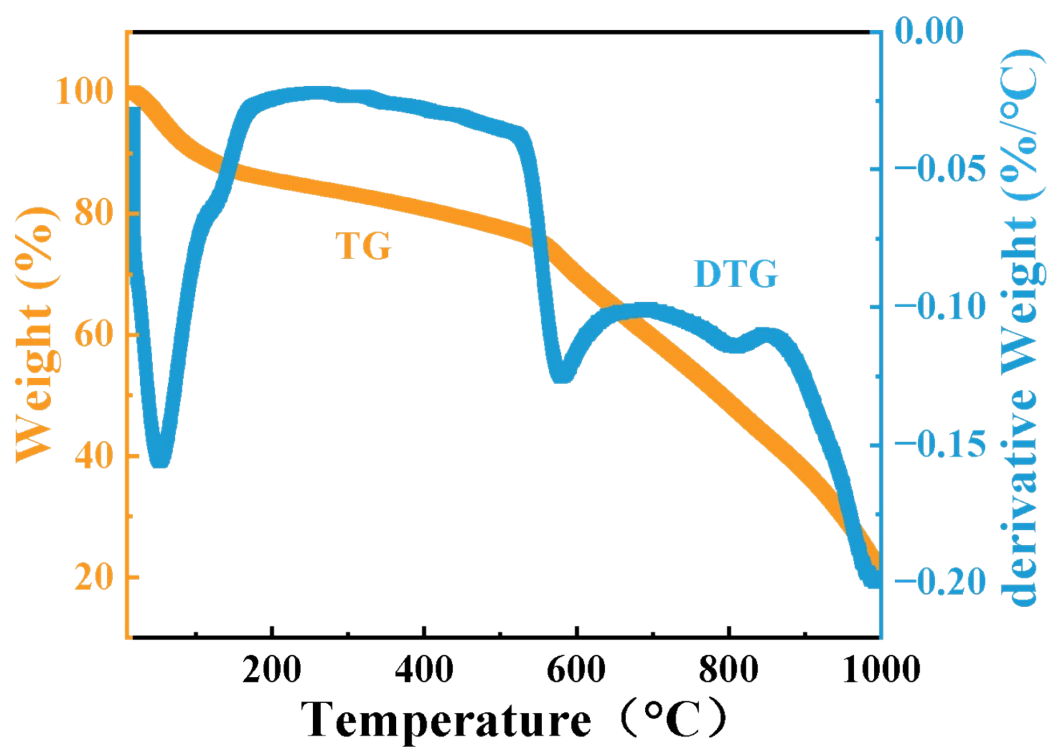


Figure S2. TG and DTG plots obtained from $\text{Co}_V\text{-N-C}_{850}$ in a N_2 atmosphere
at a heating rate of $10^{\circ}\text{C}\cdot\text{min}^{-1}$

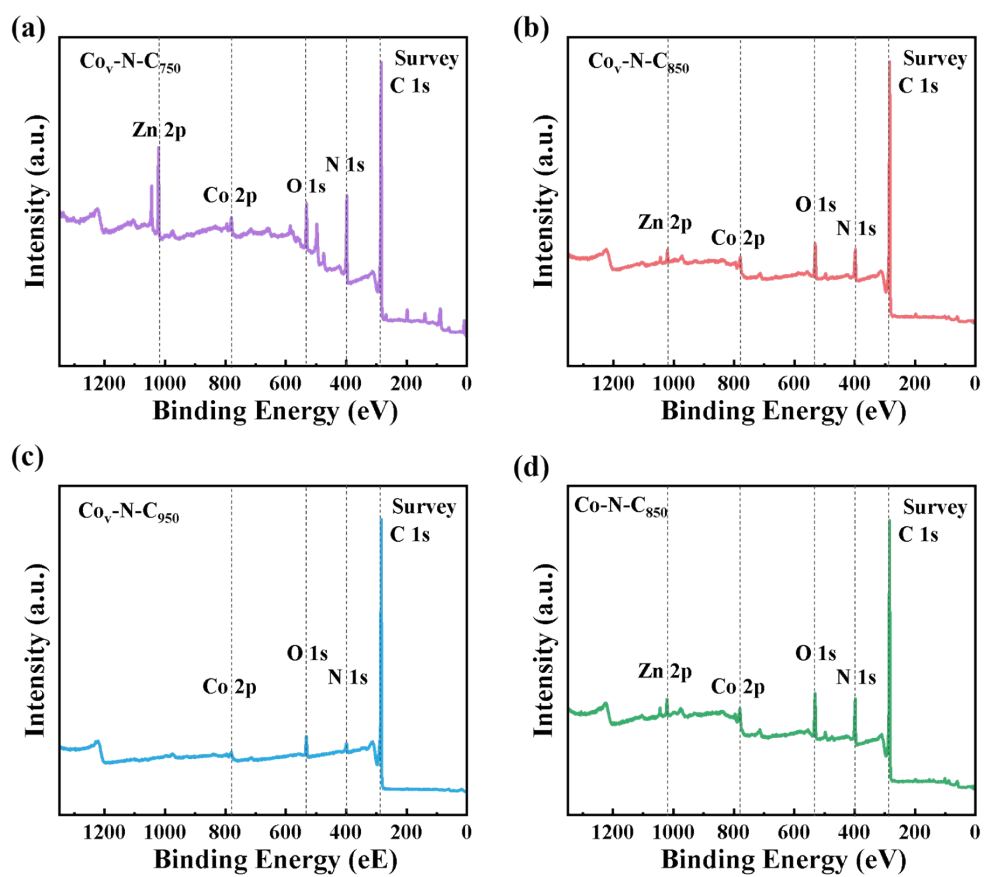


Figure S3. XPS full scan of (a) $\text{Co}_V\text{-N-C}_{750}$ (b) $\text{Co}_V\text{-N-C}_{850}$ (c) $\text{Co}_V\text{-N-C}_{950}$ (d) Co-N-C_{850}

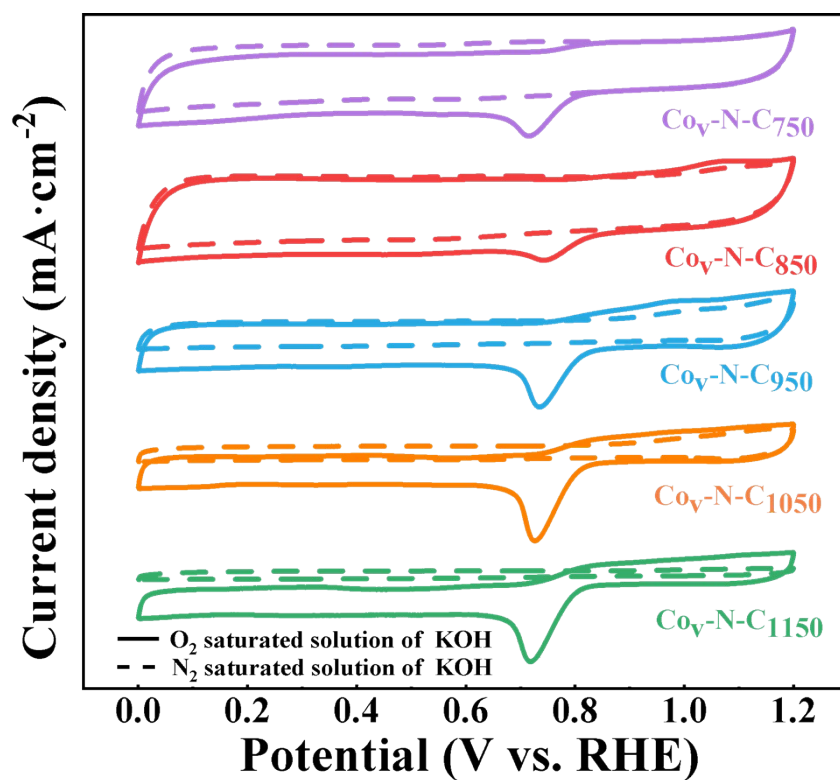


Figure S4. Cyclic voltammetry curves of Co_v-N-C₇₅₀, Co_v-N-C₈₅₀, Co_v-N-C₉₅₀, Co_v-N-C₁₀₅₀, Co_v-N-C₁₁₅₀

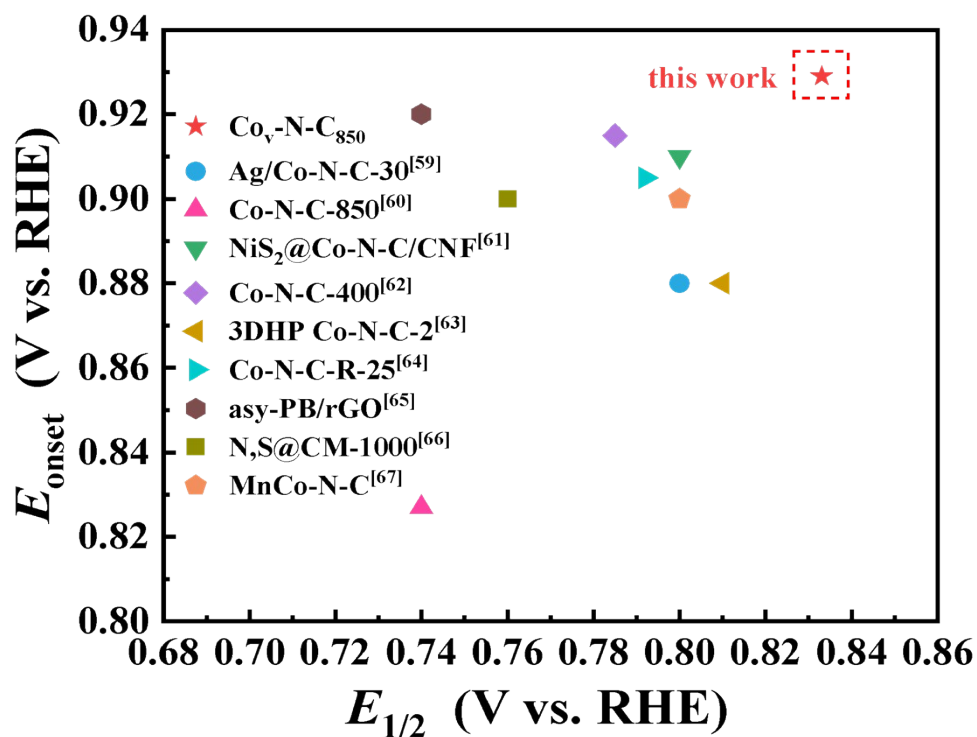


Figure S5. Comparison of ORR electrocatalytic performance of Co_v-N-C₈₅₀ with other reported non-precious and metal-free catalysts in alkaline solution

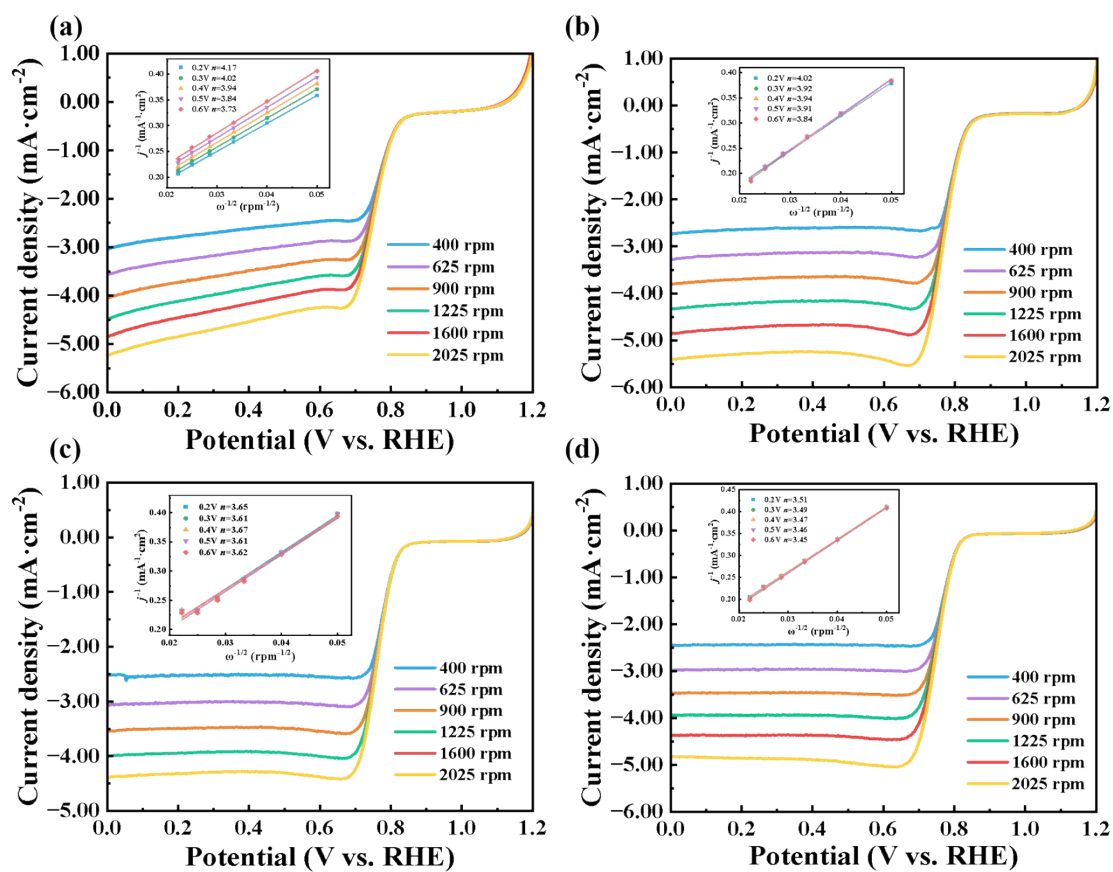


Figure S6. LSV curves of (a) Co_v-N-C₇₅₀ (b) Co_v-N-C₉₅₀ (c) Co_v-N-C₁₀₅₀ (d) Co_v-N-C₁₁₅₀ in 0.1 M O₂-saturated KOH electrolyte at different rotational speeds (from 400 to 2025 rpm) (scanning rate: 10 mV·s⁻¹)

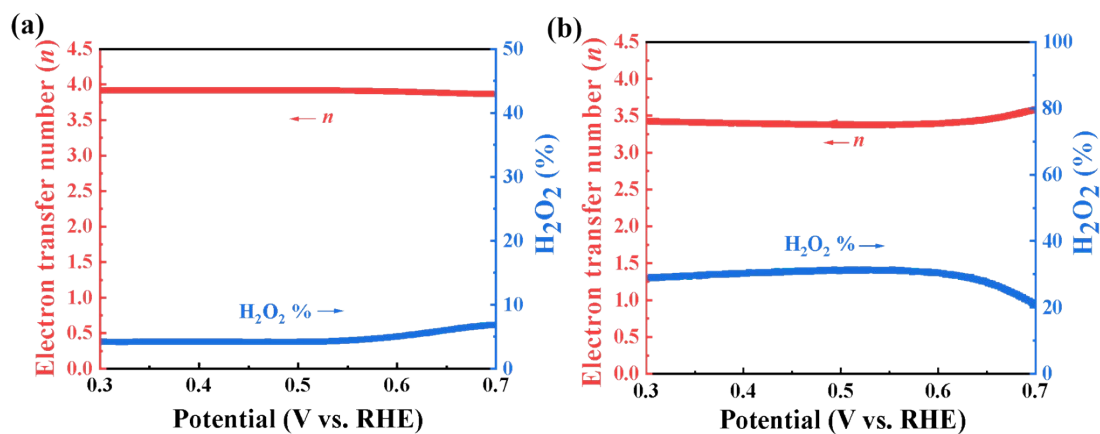


Figure S7. Hydrogen peroxide yield and electron transfer number at Pt/C and Co_v-N-C₈₅₀ electrodes

Table S1. Chemical element composition in Co-N-C catalysts

Samples	C/wt%	N/wt%	O/wt%	Co/wt%	Zn/wt%
Co _v -N-C ₈₅₀	61.01	20.83	11.11	6.48	0.58
Co-N-C ₈₅₀	60.63	19.44	8.48	9.89	1.56

Table S2. Specific surface area, microporous volume and mesopore volume of Co_v-N-C₉₅₀, Co_v-N-C₈₅₀, Co_v-N-C₇₅₀, Co-N-C₈₅₀

Samples	SBET (m ² /g)	V _{micropore} (cm ³ /g)	V _{mesopore} (cm ³ /g)
Co _v -N-C ₉₅₀	372.83	0.11	0.34
Co _v -N-C ₈₅₀	373.41	0.13	0.29
Co _v -N-C ₇₅₀	244.27	0.08	0.27
Co-N-C ₈₅₀	478.53	0.16	0.16

Table S3. ORR peak potential of Co_v-N-C₇₅₀, Co_v-N-C₈₅₀, Co_v-N-C₉₅₀, Co_v-N-C₁₀₅₀, Co_v-N-C₁₁₅₀

Samples	ORR peak potential/V (vs. RHE)
Co _v -N-C ₇₅₀	0.716
Co _v -N-C ₈₅₀	0.746
Co _v -N-C ₉₅₀	0.733
Co _v -N-C ₁₀₅₀	0.726
Co _v -N-C ₁₁₅₀	0.721

Table S4. Onset potentials, half-slope potentials and limiting current densities for LSV of different catalysts

Samples	Onset potentials (E_{onset})/V (vs. RHE)	half-slope potentials ($E_{1/2}$)/V (vs. RHE)	limiting current densities (j_L)/(mA/cm ²)
Co _v -N-C ₇₅₀	0.856	0.772	5.025
Co _v -N-C ₈₅₀	0.929	0.833	5.132
Co _v -N-C ₉₅₀	0.884	0.798	4.979
Co _v -N-C ₁₀₅₀	0.852	0.784	4.548
Co _v -N-C ₁₁₅₀	0.842	0.776	4.472
Co-N-C ₈₅₀	0.919	0.812	5.038
Pt/C (20%wt)	0.935	0.825	5.284

Table S5. Comparison of ORR electrocatalytic performance of Co_v-N-C₈₅₀ with other reported non-precious and metal-free catalysts in alkaline solution

Composite Materials	Onset potentials (E_{onset})/V (vs. RHE)	half-slope potentials ($E_{1/2}$)/V (vs. RHE)	References
------------------------	---	---	------------

Co _v -N-C ₈₅₀	0.929	0.833	\
Ag/Co-N-C-30	0.88	0.80	[59]
Co-N-C-850	0.827	0.74	[60]
NiS ₂ @Co-N-C/CNF	0.91	0.80	[61]
Co-N-C-400	0.915	0.785	[62]
3DHP Co-N-C-2	0.88	0.81	[63]
Co-N-C-R-25	0.905	0.792	[64]
asy-PB/rGO	0.92	0.74	[65]
N,S@C _M -1000	0.90	0.76	[66]
MnCo-N-C	0.90	0.80	[67]

Table S6. Internal resistance and charge transfer resistance of Co_v-N-C₇₅₀, Co_v-N-C₈₅₀, Co_v-N-C₉₅₀, Co_v-N-C₁₀₅₀, Co_v-N-C₁₁₅₀

Samples	Internal resistance (R_1) (Ω)	charge transfer resistance (R_{ct}) (Ω)
Co _v -N-C ₇₅₀	32.42	912.4
Co _v -N-C ₈₅₀	30.2	176.4
Co _v -N-C ₉₅₀	32.45	512.7
Co _v -N-C ₁₀₅₀	30.2	1248
Co _v -N-C ₁₁₅₀	31.99	3735